Cellular and Molecular Life Sciences (2018) 75:3027–3038
https://doi.org/10.1007/s00018-018-2777-0

ORIGINAL ARTICLE

Conformational change of the extracellular parts of the CFTR protein during channel gating

Alexander Negoda[1] · Elizabeth A. Cowley[1] · Yassine El Hiani[1] · Paul Linsdell[1]

Received: 28 November 2017 / Revised: 24 January 2018 / Accepted: 8 February 2018 / Published online: 14 February 2018

Abstract

Cystic fibrosis can be treated by potentiators, drugs that interact directly with the cystic fibrosis transmembrane conductance regulator (CFTR) Cl^- channel to increase its open probability. These substances likely target key conformational changes occurring during channel opening and closing, however, the molecular bases of these conformational changes, and their susceptibility to manipulation are poorly understood. We have used patch clamp recording to identify changes in the three-dimensional organization of the extracellularly accessible parts of the CFTR protein during channel opening and closing. State-dependent formation of both disulfide bonds and Cd^{2+} bridges occurred for pairs of cysteine side-chains introduced into the extreme extracellular ends of transmembrane helices (TMs) 1, 6, and 12. Between each of these three TMs, we found that both disulfide bonds and metal bridges formed preferentially or exclusively in the closed state and that these inter-TM cross-links stabilized the closed state. These results indicate that the extracellular ends of these TMs are close together when the channel is closed and that they separate from each other when the channel opens. These findings identify for the first time key conformational changes in the extracellular parts of the CFTR protein that can potentially be manipulated to control channel activity.

Keywords Cystic fibrosis transmembrane conductance regulator · Chloride channel · Cysteine cross-linking · Conformational change · Potentiator · Channel structure

Abbreviations

ABC	ATP-binding cassette
CF	Cystic fibrosis
CFTR	CF transmembrane conductance regulator
CHO	Chinese hamster ovary
cryo-EM	Cryo-electron microscopy
CuPhe	Copper(II)-*o*-phenanthroline
DTT	Dithiothreitol
ECL	Extracellular loop
NBD	Nucleotide-binding domain
TM	Transmembrane helix

Introduction

Cystic fibrosis (CF) is caused by mutations in the CF transmembrane conductance regulator (CFTR), an epithelial cell Cl^- channel. Because CFTR dysfunction is the root cause of CF, there is great interest in the development of so-called potentiator drugs that interact directly with CFTR to increase its function [1, 2]. As an ion channel, an increase in CFTR function would be reflected in an increase in the proportion of time the channel spends in the open, conducting state relative to the closed, non-conducting state (often referred to as channel open probability). Drugs that interact with CFTR to increase the stability of the open state (impair the conformational change to the closed state) and/or decrease the stability of the closed state (facilitate the conformational change to the open state) should, therefore, exhibit potentiator function. It is important, therefore, to understand how these conformational changes between states take place, and in particular, those localized changes in conformation that might be manipulated to increase overall channel open probability [3–5].

✉ Paul Linsdell
paul.linsdell@dal.ca

[1] Department of Physiology and Biophysics, Dalhousie University, PO Box 15000, Halifax, NS B3H 4R2, Canada

CFTR channel activity requires phosphorylation by protein kinase A, following which channel opening and closing is controlled by ATP interaction with the two cytoplasmic nucleotide-binding domains (NBDs) [4, 5]. Functional evidence suggests that, following ATP-dependent NBD dimerization, a propagated conformational change is transmitted via intracellular loops of the protein towards the transmembrane α-helices (TMs), resulting in the opening of a "gate" located near the extracellular ends of the TMs [3, 6–8]. Consistent with this model, the structure of CFTR observed by cryo-electron microscopy (cryo-EM) in the dephosphorylated, inactive state (Fig. 1) shows widely separated NBDs [10], whereas the cryo-EM structure in a "near-open" state that is closed only at the extracellular end of the TMs (Fig. 1) shows dimerized NBDs [11]. Based on differences between these two structures, it was proposed that channel opening and closing is associated with a rigid-body movement of the TMs [11]. However, the extent to which these two static structures reflect the dynamic changes that must occur during normal opening and closing of the channel pore is not currently clear [4, 11, 12].

Of those conformational changes proposed to take place during channel opening and closing [3], which might be manipulated by small drugs to influence overall channel activity? Previously, we identified separation and convergence of different TMs as important structural rearrangements taking place during channel gating, and showed that interfering with the relative movement of different TMs can directly alter the stability of the open and closed states [13].

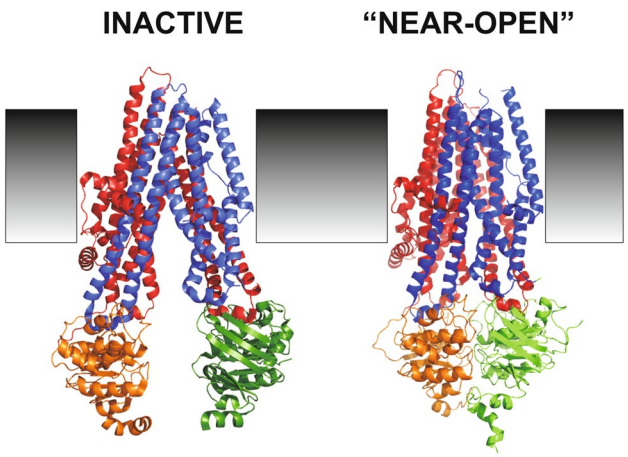

Fig. 1 Structure of CFTR in different conformations. The structure of CFTR has recently been observed using cryo-EM under conditions expected to result in different conformational states of the protein. Left, human CFTR in the inactive, dephosphorylated state [10]. Right, zebrafish CFTR in a "near-open" state in which the pore is closed only at the extracellular ends of the TMs [11]. In these models, the first membrane-spanning domain (TMs 1–6) is red, the second membrane-spanning domain (including TMs 7–12) is blue, NBD1 is orange, and NBD2 is green

These findings offer encouragement that the TMs themselves might be possible sites at which small molecules could directly potentiate CFTR channel activity [3].

The most accessible part of the TMs is their extracellular ends that are exposed to the outside of the cell (Fig. 1). On the extracellular side, the TMs are connected by extracellular loops (ECLs), most of which are very short. Using functional approaches, several TMs/ECLs have been shown to be accessible from the extracellular solution, and to contribute to the outermost part of the Cl^- permeation pore, including TM1/ECL1, ECL3/TM6, and ECL6/TM12 [14]. Furthermore, important changes in conformation have been proposed for this part of CFTR during channel gating. For example, it has been reported by several groups that access from the extracellular solution to the outer part of the pore is greater when the channel is closed and paradoxically decreases when the channel opens [8, 15–18]. Based on these findings, we suggested that the outer mouth of the pore might physically constrict when the channel opens [3, 17]. To investigate conformational changes at the extracellular mouth of the pore during gating, we have now sought to engineer disulfide bonds and Cd^{2+} bridges between cysteine side-chains introduced at the outer ends of different TMs. We find that both disulfide bonds and Cd^{2+} bridges can be formed between each of TMs 1, 6, and 12. However, in all cases, these inter-TM interactions appear to occur preferentially in the closed state. We propose that the outer ends of the TMs are in close proximity in closed channels and that they separate from each other when the channel opens.

Materials and methods

Experiments were carried out on Chinese hamster ovary (CHO) cells transiently transfected with human CFTR, using procedures similar to those described previously [19]. The CFTR variant used was a so-called "cys-less" CFTR in which all cysteines have been removed by mutagenesis [20] and includes a mutation in the first NBD (V510A) to increase protein expression in the cell membrane [21]. Additional mutations were introduced using the QuikChange site-directed mutagenesis system (Agilent Technologies, Santa Clara, CA, USA) and verified by DNA sequencing. Cysteine residues were substituted at sites at the extracellular ends of TM1 (R104, I106), TM6 (K329, I331, L333), and TM12 (G1127, V1129, I1131) that have previously been shown to be accessible to cysteine-reactive reagents in the extracellular solution [16, 22–24]. In some cases, cysteine substitutions were combined with the NBD2 mutation E1371Q, since mutation of this important glutamate residue results in near-permanently open channels [25]. Previously, we have used the E1371Q mutation to study the channel state

dependence of the proximity of cysteine residues introduced into different parts of CFTR [13, 18].

The proximity of pairs of cysteine side-chains introduced into different TMs was identified functionally using patch clamp recording, in two different ways. First, formation of disulfide bonds between two cysteine side-chains was inferred from changes in current amplitude resulting from treatment with the oxidizing agent copper(II)-*o*-phenanthroline (CuPhe) [18, 26, 27]. Since disulfide formation results in covalent attachment of two cysteines that is essentially irreversible under oxidizing conditions, this approach was used as a first screen to test which cysteine pairs showed close proximity at some stage during normal channel activity. Second, Cd^{2+} ions were used to form metal bridges between pairs of cysteine side-chains [13]. Because Cd^{2+} bridge formation is reversible, this approach is of greater utility in studying state-dependent changes in the proximity of pairs of cysteine side-chains, from changes in apparent Cd^{2+}-binding affinity under different gating conditions [13, 28]. For experiments using either CuPhe or Cd^{2+} exposure, cells were pre-treated with dithiothreitol (DTT; 5 mM) for 5 min immediately prior to the experiment, to ensure that cysteine side-chains were in a reduced state.

Whole-cell patch clamp recordings were made as described previously [27]. Briefly, bath (extracellular) solution contained (mM): 145 NaCl, 15 Na glutamate, 4.5 KCl, 1 $MgCl_2$, 2 $CaCl_2$, 10 HEPES, 5 glucose, pH 7.4, and pipette (intracellular) solution contained (mM): 139 CsCl, 2 $MgCl_2$, 5 EGTA, 10 HEPES, 5 glucose, 4 Na_2ATP, 1 MgATP, 0.1 GTP, pH 7.2. Following attainment of the whole-cell configuration and recording of stable baseline currents, CFTR channels were activated by extracellular application of a cyclic AMP stimulatory cocktail containing forskolin (10 μM), 3-isobutyl-1-methylxanthine (100 μM), and 8-(4-chlorophenylthio) cyclic AMP (100 μM). At the end of the experiment, remaining currents were confirmed as being carried by CFTR by their sensitivity to the specific CFTR inhibitor GlyH-101. CFTR channel currents were monitored during depolarizing voltage ramps (from − 50 to + 50 mV) applied every 10 s. CuPhe was prepared freshly before each experiment by mixing stock solutions of $CuSO_4$ (200 mM in distilled water) with 1,10-phenanthroline (200 mM in ethanol) in a 1:4 molar ratio. A low final concentration of 10 μM Cu^{2+}:40 μM phenanthroline was applied to cells to minimize the potential for non-specific effects [27]. Indeed, this concentration of CuPhe was found to be without effect on mutants containing only a single-cysteine residue at any of the sites investigated in this study (data not shown). Different concentrations of $CdCl_2$ were applied to cells from stock solutions made up in normal extracellular solution. The relationship between $[Cd^{2+}]$ and inhibition of current amplitude was fitted by the equation:

$$\text{Fractional unblocked current} = 1/(1 + ([Cd^{2+}]/K_i)).$$

Experiments were carried out at room temperature, 21–24 °C. Values are presented as mean ± SEM. For graphical presentation of mean values, error bars represent SEM. Where no error bars are visible, SEM is smaller than the size of the symbol. Tests of significance were carried out using Student's two-tailed *t* test, with $p < 0.05$ being considered statistically significant. All chemicals were from Sigma-Aldrich (Oakville, ON, Canada) except for GlyH-101 (EMD Chemicals, Gibbstown, NJ, USA).

Results

Disulfide bond formation between the extracellular ends of different TMs

To test for physical proximity between the outer ends of different TMs, we constructed mutant channels with one externally accessible cysteine in TM6 (K329C, I331C, L333C) as well as one in TM12 (G1127C, V1129C, I1131C)—a total of nine double-cysteine mutant channels. As in our previous work [27], the ability of these pairs of cysteines to form disulfide bonds was then investigated using whole-cell patch clamp recording (Fig. 2). Following channel activation using cAMP, cells were treated with CuPhe to catalyze the formation of disulfide bonds (Fig. 2a, b). In seven of the nine cases tested, treatment with CuPhe caused a decrease in current amplitude (Fig. 2a–c) that could be at least partially reversed by the addition of DTT (Fig. 2a). These results are consistent with cysteine side-chains at several positions at the extracellular extremes of these two TMs being able to form inter-TM disulfide bonds that impair channel function in some way.

We used a similar approach to test the proximity of the outer end of TM1 to both TM6 and TM12. Cysteines were introduced at two externally accessible sites in TM1 (R104C, I106C) in combination with the above-listed sites in TM6 and TM12 (an additional 12 double-cysteine mutant channel constructs). One of these mutants (I106C/L333C) did not yield cAMP-activated currents when expressed in CHO cells, in spite of several independent attempts to generate this channel construct. However, the other eleven mutants did generate currents that in several cases were reduced in amplitude following exposure to CuPhe, with this apparent inhibition at least partially reversed by DTT (Fig. 3). Again, this is consistent with the formation of inter-TM disulfide bonds between TM1 and either TM6 or TM12 that inhibit channel function.

One interpretation of the inhibitory effects of CuPhe that we commonly observed in channels containing cysteines in TM6 and TM12 (Fig. 2), TM1 and TM6 (Fig. 3), and TM1 and TM12 (Fig. 3) is that formation of disulfide bonds between these TMs constrains the channel in the closed state. If true, this would suggest that the outer ends of each

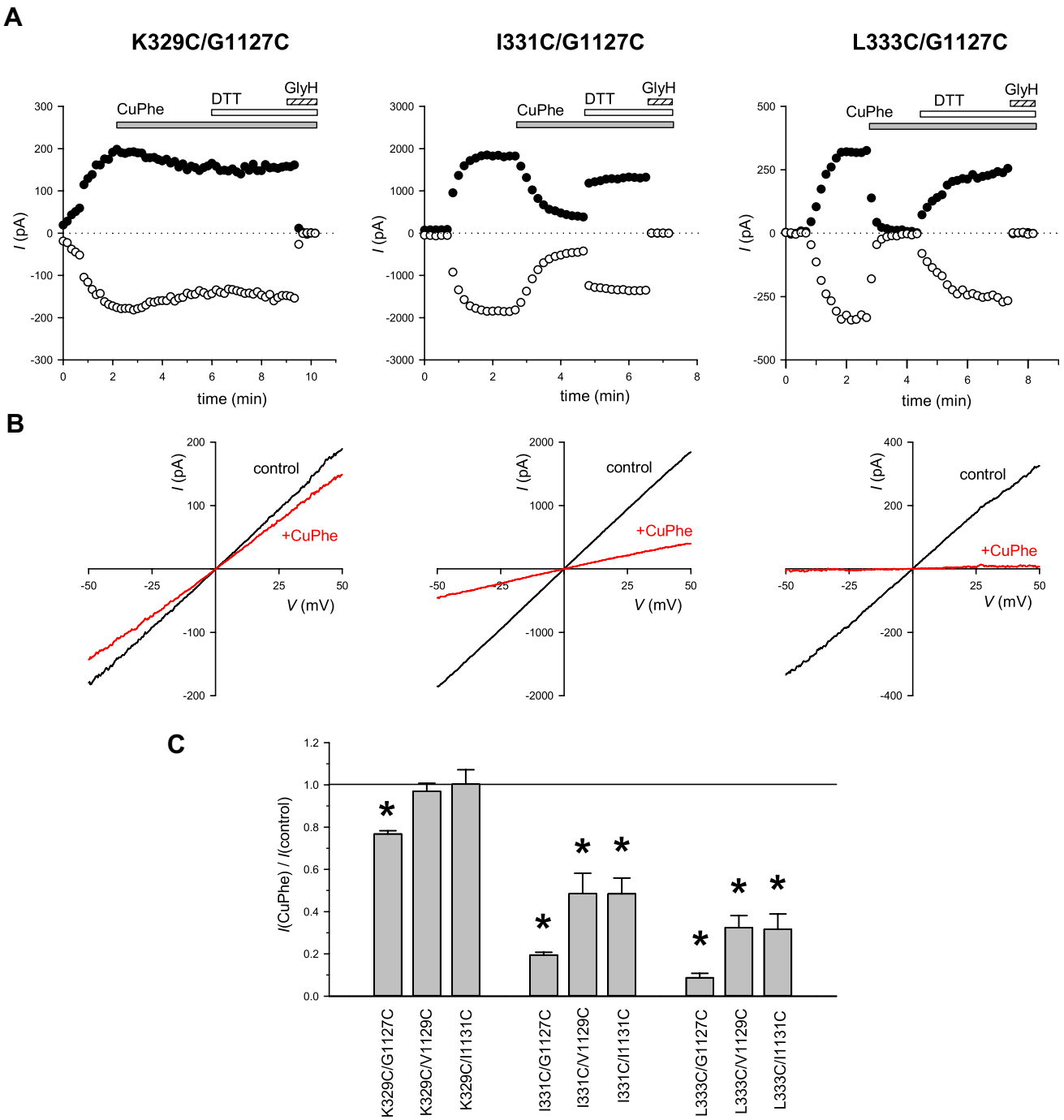

Fig. 2 Disulfide bond formation between the outer ends of TM6 and TM12. **a** Examples of the timecourse of whole-cell currents carried by different channel variants bearing one cysteine residue in TM6 and one in TM12. As described in "Materials and methods", the current amplitude was monitored using voltage ramps (**b**) and is plotted at membrane potentials of − 50 mV (open circles) and + 50 mV (filled circles). Currents were activated at or just after time zero by extracellular application of cAMP stimulatory cocktail. After activation, cells were treated sequentially with CuPhe (10 µM Cu^{2+}: 40 µM phenanthroline; grey bars) and DTT (5 mM; white bars). At the end of the experiment, current was confirmed as CFTR using GlyH-101 (20 µM; hatched bars marked GlyH). **b** Example current (*I*)–voltage (*V*) relationships for these cells, recorded during voltage ramps before (control; black lines) and after (red lines) treatment with CuPhe. **c** Mean effect of CuPhe application on whole-cell current amplitude in these and other cysteine double mutant channels. Asterisks indicate those variants in which CuPhe application resulted in a significant change in the current amplitude ($p < 0.05$). Mean of data from 3 to 7 cells

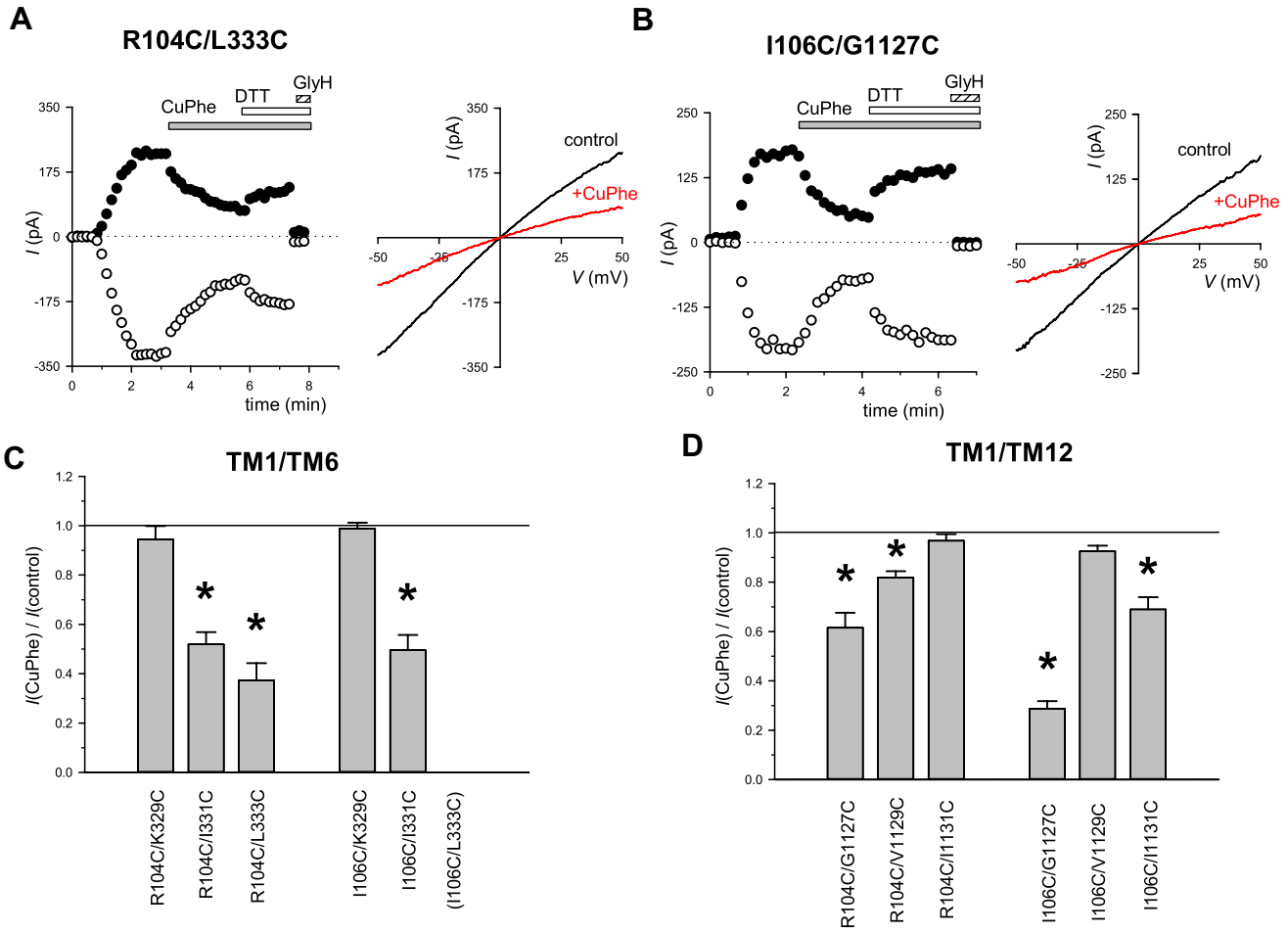

Fig. 3 Disulfide bond formation between the outer end of TM1 and TMs 6 or 12. Example whole-cell currents carried by R104C/L333C (**a**) and I106C/G1127C (**b**) channels, under conditions identical to those used in Fig. 2. Mean effect of CuPhe application on whole-cell current amplitude in channel variants bearing one cysteine in TM1, together with one cysteine in either TM6 (**c**) or in TM12 (**d**). In both cases, asterisks indicate those variants in which CuPhe application resulted in a significant change in current amplitude ($p < 0.05$). Note that no whole-cell current was observed in cells transfected with I106C/L333C DNA. Mean of data from 3 to 4 cells in **c** and **d**

of these TMs are closer together when the channel is closed than when it is open. To investigate this possibility further, we investigated disulfide bond formation in channels bearing the E1371Q mutation in NBD2. This mutation has been shown to result in channels that are almost permanently open [18]. In each of three cysteine pairs that carried current that was strongly inhibited by CuPhe—namely, I331C/G1127C (TM6:TM12; Fig. 2), L333C/G1127C (TM6:TM12; Fig. 2), and R104C/L333C (TM1:TM6; Fig. 3a, c)—we found that the E1371Q mutation significantly reduced the inhibitory effects of exposure to CuPhe (Fig. 4). This suggests that disulfide bonds formed less readily (if at all) in these channel constructs in the open state, which further suggests that disulfide bond formation normally occurs preferentially (or perhaps exclusively) in the closed state. In contrast, in a fourth strongly CuPhe-sensitive mutant (I106C/G1127C, TM1:TM12; Fig. 3b, d), the E1371Q mutation had no significant effect on the extent of current inhibition caused by CuPhe (Fig. 4), suggesting that disulfide bonds form readily between these two cysteines in the open state.

Metal bridge formation between the extracellular ends of different TMs

To further investigate the potential state-dependent proximity of cysteine side-chains introduced at the extracellular ends of different TMs, we used extracellular application of Cd^{2+} ions to form metal bridges between cysteine side-chains [28]. Figure 5 shows the effect of Cd^{2+} on currents carried by two channel variants bearing cysteines in TMs 6 and 12 that were strongly inhibited by CuPhe exposure, I331C/G1127C and L333C/G1127C (Figs. 2, 4), as well as single-cysteine control channels I331C and L333C (G1127C alone was not noticeably sensitive to Cd^{2+} even

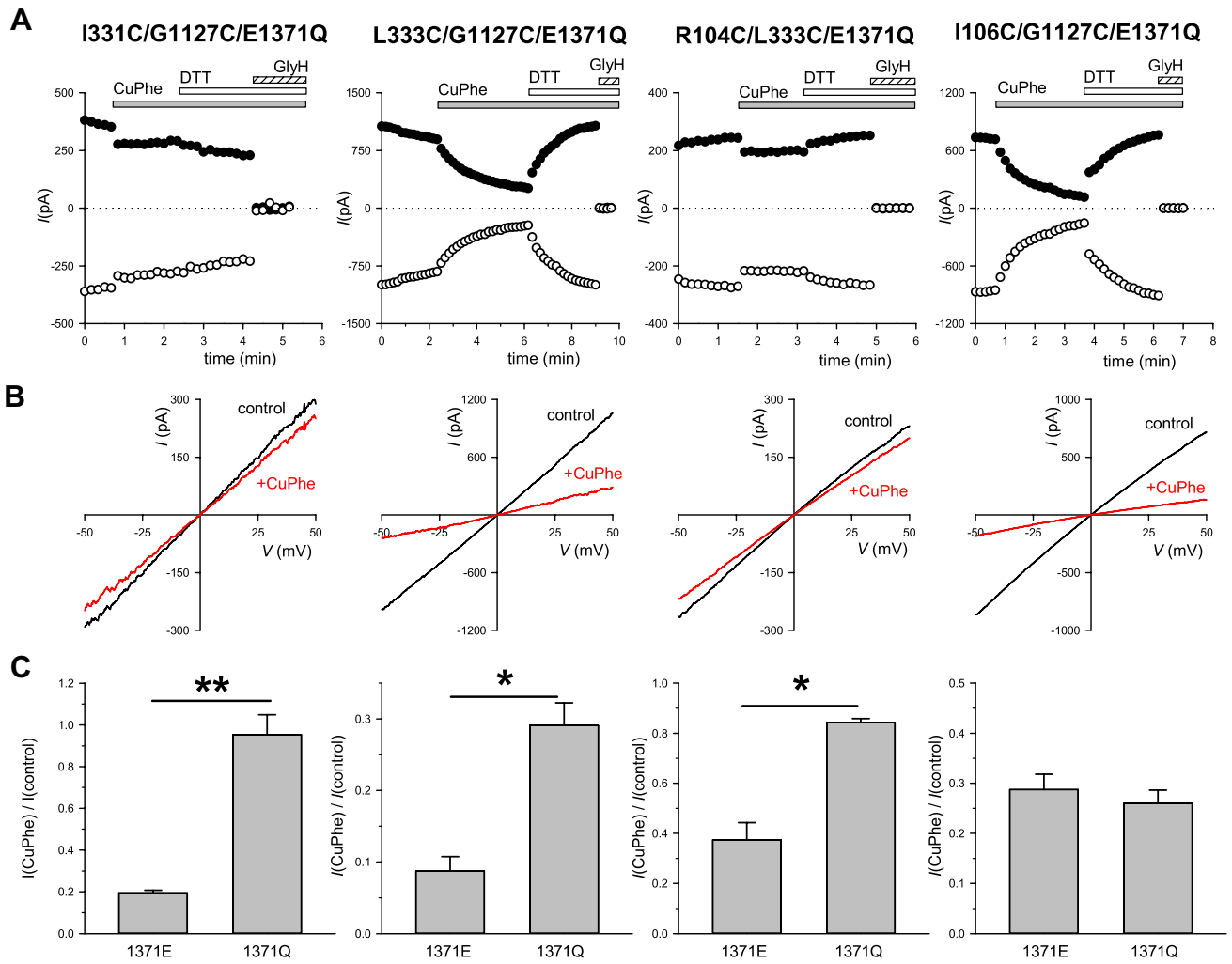

Fig. 4 Altered disulfide bond formation in permanently open channels. **a**, **b** Example whole-cell currents carried by four different channel variants, each bearing two cysteine residues in a permanently open E1371Q background (as indicated), under experimental conditions identical to those used in Fig. 2. **c** Mean effect of CuPhe application on whole-cell current amplitude in these channel variants (1371Q) compared to those lacking the E1371Q mutation (1371E; data taken from Figs. 2 and 3). Asterisks indicate a significant difference in the effect of CuPhe between corresponding 1371Q and 1371E variants (*$p < 0.001$; **$p < 0.00001$). Mean of data from 3 to 7 cells

at concentrations as high as 100 µM). In each of these mutants, whole-cell current was inhibited in a concentration-dependent fashion by extracellular Cd^{2+}. Currents carried by I331C/G1127C, as well as I331C/G1127C/E1371Q, were not significantly more sensitive to Cd^{2+} than was the single I331C mutant (Fig. 5a, c, e), perhaps due to the unusually strong inhibition of I331C by Cd^{2+} (K_i ~ 5 µM; Fig. 5e). In contrast, L333C/G1127C channels exhibited a very high apparent affinity for Cd^{2+} ions (K_i ~ 40 nM; Fig. 5f) that was more than 4000-fold higher than that of L333C (Fig. 5c, f), suggesting very strong coordination of Cd^{2+} ions by two proximal cysteine side-chains introduced at positions 333 and 1127. Interestingly, the high apparent affinity of Cd^{2+} ions for this pair of cysteine side-chains was reduced by approximately 35-fold by the E1371Q mutation (Fig. 5d, f). Assuming that the effect of Cd^{2+} on L333C/G1127C/E1371Q channels reflects Cd^{2+} binding to the channel open state, this result suggests that Cd^{2+} binds these two cysteine side-chains with much greater affinity in the channel closed state than in the open state.

Similar experiments on strongly CuPhe-sensitive mutants with cysteines in TM1 (R104C/L333C, TM1:TM6; I106C/G1127C, TM1:TM12; Figs. 2, 4) are shown in Fig. 6. Again, double-cysteine mutants were strongly inhibited by extracellular Cd^{2+} compared to single-cysteine control mutants (Fig. 6), with apparent K_is of ~ 13 µM for R104C/L333C (Fig. 6e) and ~ 100 nM for I106C/G1127C (Fig. 6f), again consistent with strong Cd^{2+} coordination by proximal cysteine side-chains. As with L333C/G1127C described above (Fig. 5), the affinity of Cd^{2+} binding was significantly

reduced by the E1371Q mutation, by approximately fourfold in R104C/L333C/E1371Q (Fig. 6e) and approximately sevenfold in I106C/G1127C/E1371Q (Fig. 6f). As described above, this finding is consistent with these two pairs of cysteine side-chains binding Cd^{2+} with higher affinity in the closed state compared with the open state.

Discussion

Functional evidence suggests that residues near the extracellular ends of TMs 1, 6, and 12 lie close to the extracellular entrance to the CFTR channel pore [12]. Our present results show that the extracellular ends of these TMs are close enough together for disulfide bonds to form between cysteine side-chains introduced into each of these TMs (Figs. 2, 3). Formation of disulfide bonds between two cysteine side-chains is generally considered to require S–S distances of ~ 2 Å, with the Cβ–Cβ distance 3.4–4.6 Å and the Cα–Cα distance ~ 3.8–6.8 Å [28], which, therefore, places important structural constraints on the outermost part of the pore (Fig. 7). Strong apparent coordination of Cd^{2+} ions by many of these same cysteine pairs (Figs. 5, 6) also suggests close physical proximity [28]. Interestingly, disulfide bonds and Cd^{2+} bridges could be formed between individual cysteine residues and multiple partners (for example, G1127C can form such interactions with I106C, I331C, and L333C), even when these partners appear several Å apart in the static cryo-EM structure (Fig. 7). This could reflect dynamic structural flexibility in this part of CFTR, emphasizing that the positions of specific side-chains reported in static structures such as cryo-EM should be considered as, at best, the average of conformational ensembles.

In fact, our results suggest that the outer ends of TMs 1, 6, and 12 are closer together when the channel is closed and that they move farther apart when the channel opens. The most direct evidence for such state-dependent changes in proximity come from the effect of the E1371Q mutation on the coordination of Cd^{2+} ions by two cysteine side-chains (Figs. 5, 6). In the most extreme case (L333C/G1127C), the introduction of the E1371Q mutation reduced apparent Cd^{2+}-binding affinity by approximately 35-fold (Fig. 5d, f). If lower affinity Cd^{2+} binding to E1371Q-containing channels is assumed to reflect Cd^{2+} binding to the open state, then the affinity of Cd^{2+} binding must increase greatly when the channels close, suggesting much stronger Cd^{2+} coordination by closed channels than by open channels. The most likely explanation is that these two cysteine side-chains move close together when the channel closes (to allow tight Cd^{2+} coordination) and that they separate somewhat when the channel opens (resulting in a weakening of Cd^{2+} coordination). Qualitatively similar, although somewhat less striking, results were found with R104C/L333C (Fig. 6c, e) and I106C/G1127C (Fig. 6d, f), again consistent with these side-chains moving apart when the channel opens. In contrast, we found no evidence for Cd^{2+} bridge formation between I331C and G1127C (Fig. 5c, e), in spite of the fact that disulfide bonds apparently form readily between two cysteines at these positions (Fig. 2). As discussed below, we believe that any potential Cd^{2+} bridge formation between these two side-chains may be masked by the very high apparent Cd^{2+}-binding affinity of the I331C side-chain in isolation (Fig. 5a, c, e). In all cases where there is evidence for Cd^{2+} bridge formation—between TM1 and TM6 (R104C/L333C; Fig. 6c, e), between TM1 and TM12 (I106C/G1127C; Fig. 6d, f), and between TM6 and TM12 (L333C/G1127C; Fig. 5d, f)—Cd^{2+} bridge formation inhibits channel function, consistent with these Cd^{2+} bridges acting to stabilize the closed state. Since Cd^{2+} interacts more strongly with the closed state, its inhibitory effects on channel function presumably reflect changes in channel gating rather than inhibition of Cl^- permeation through the open channel. The consistent stabilization of the closed state observed in the present study contrasts with our earlier finding that a Cd^{2+} bridge between residues located in the inner vestibule of the pore, between TM1 (K95C) and TM12 (S1141C), acts to stabilize the channel open state [13]. In the present study, at those sites that were tested, we found no evidence for Cd^{2+} bridges that could stabilize the open state.

We found that all constructs tested with a cysteine substituted for I331 were potently inhibited by low concentrations of Cd^{2+} (Fig. 5a, c, e). Indeed, I331C itself was strongly inhibited by Cd^{2+} (K_i ~ 5 μM), in contrast with other single-cysteine mutants with K_is > 100 μM (Figs. 5, 6) which is more typical for Cd^{2+} interaction with a single-cysteine side-chain [28]. One possible explanation for this result is that Cd^{2+} might be strongly coordinated by I331C and another, nearby side-chain. While the use of cys-less CFTR ensures that there are no other cysteine side-chains present, it has been shown that Cd^{2+} ions can be coordinated by cysteine and other side-chains such as histidine, aspartate, or glutamate [29–31]. However, the possibility that such side-chains might exist in close proximity to I331C was not investigated directly.

Consistent with the suggestion that Cd^{2+} bridges could be formed more readily in the closed state, we also found that the functional effects of disulfide bond formation between cysteine side-chains in different TMs were significantly reduced by introduction of the E1371Q mutation (Fig. 4). We believe the most likely explanation is that disulfide bonds form less readily in the open state, which again is consistent with TMs approaching closer together in the closed state and moving apart in the open state. In fact, in two double-cysteine mutants studied—I331C/G1127C and R104C/L333C—CuPhe had only very small effects in the presence of the E1371Q mutant, even though it strongly

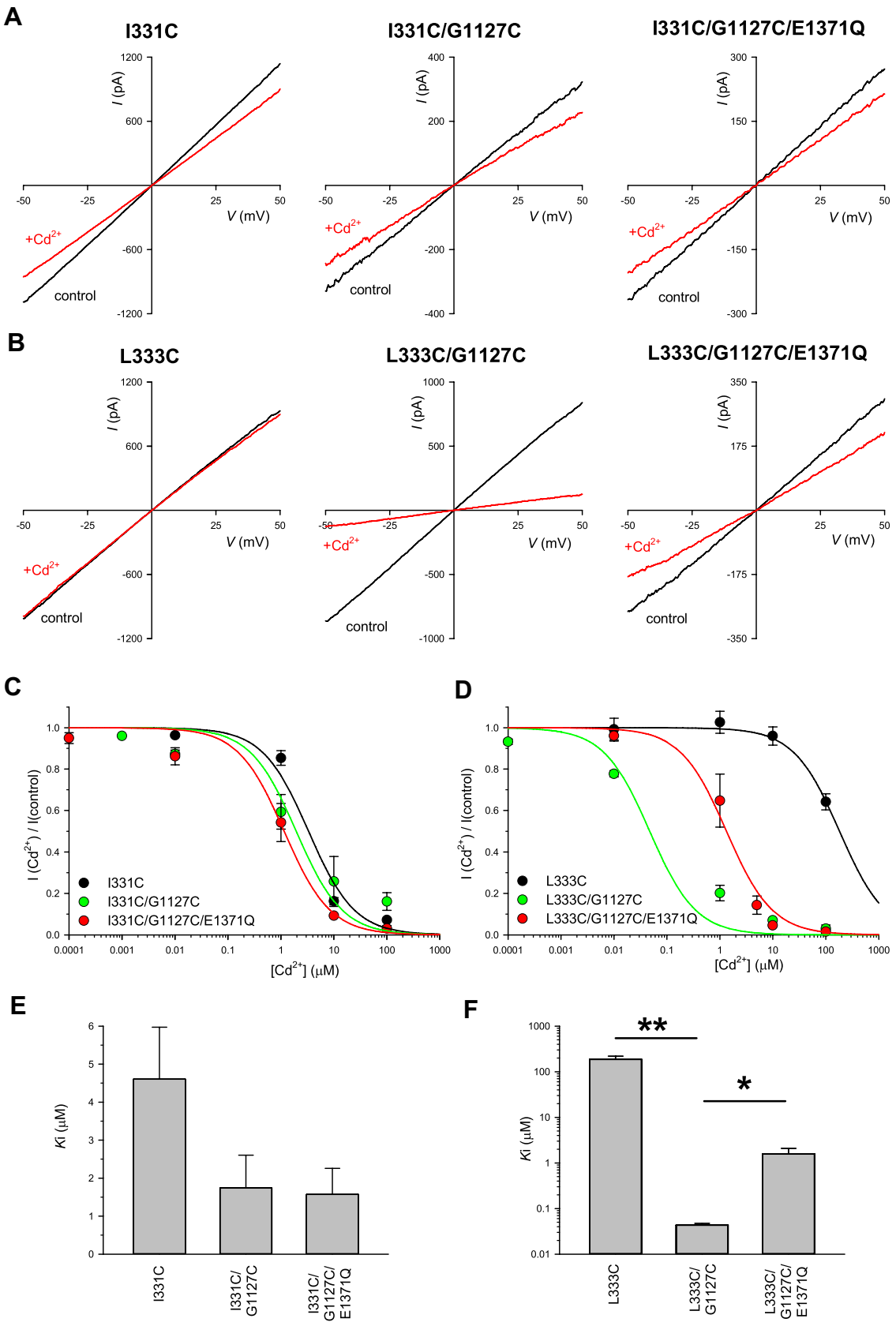
A
I331C
I331C/G1127C
I331C/G1127C/E1371Q
I (pA)
V (mV)
+Cd2+
control
B
L333C
L333C/G1127C
L333C/G1127C/E1371Q
C
I (Cd2+) / I(control)
[Cd2+] (μM)
I331C
I331C/G1127C
I331C/G1127C/E1371Q
D
L333C
L333C/G1127C
L333C/G1127C/E1371Q
E
Ki (μM)
I331C
I331C/ G1127C
I331C/ G1127C/ E1371Q
F
**
*
L333C
L333C/ G1127C
L333C/ G1127C/ E1371Q

◂**Fig. 5** State-dependent metal bridge formation between the outer ends of TM6 and TM12. **a**, **b** Example whole-cell current (*I*)–voltage (*V*) relationships for the named channel variants. Each was recorded before (control; black lines) and after (red lines) addition of Cd^{2+} (1 μM) to the extracellular solution. **c**, **d** Mean fraction of control current remaining following addition of different concentrations of Cd^{2+} to the extracellular solution for the different channel variants indicated. Mean data have been fitted as described in "Materials and methods". **e**, **f** Mean K_i values estimated from fits to data from individual cells exposed to different concentrations of Cd^{2+}. Note that the *ordinate* has a linear scale in **e** (to emphasize similarities in K_i between different channel variants) but a logarithmic scale in **f** (to emphasize large differences in K_i between channel variants). Asterisks indicate a significant difference between the groups indicated (*$p < 0.05$; **$p < 0.01$). Mean of data from 3 to 4 cells in **c**–**f**

inhibited current in 1371E-background channels that presumably were opening and closing during the experiment (Figs. 2, 3, 4). In these two cases, therefore, it is plausible that disulfide bonds cannot form in the open state but only in the closed state, consistent with a relative movement of the two cysteine side-chains in question during channel gating. Significant effects of the E1371Q mutation on sensitivity to CuPhe were also observed for R104C/L333C-bearing cysteines in TMs 1 and 6 (R104C/L333C), again consistent with the outer ends of these TMs all moving apart from each other when the channel opens. In contrast, disulfide bonds apparently formed readily between I106C (TM1) and G1127C (TM12) in the open state, suggesting that the outer ends of these TMs remain close together in open channels.

Apparent separation of the outer ends of TMs 1, 6, and 12 suggests that the outermost part of the channel pore exhibits a relatively "closed" conformation when the channel is closed and that it undergoes a relative opening transition when the channel as a whole opens (Fig. 7). Those residues at the far extracellular limits of these three TMs shown in Fig. 7a may be close enough together for disulfide bond formation when the channel is closed (although not necessarily when the channel is open), which as described above places important structural constraints on the physical dimensions of the extracellular part of the pore when the channel is closed. This close approach of the outer ends of pore-forming TMs in the closed state might be considered consistent with the existence of a functional "gate" that controls opening and closing, located relatively close to the extracellular ends of the TMs [3, 8, 9, 32]. However, it would seem to refute our previous suggestion [3, 17] that the outer mouth of the pore physically constricts during channel opening. This apparent discrepancy might suggest that reduced accessibility to residues in the outer part of the pore during channel opening could reflect not overall pore constriction, but other, more specifically localized changes in pore architecture. It has been suggested that individual TMs might undergo translational [18] and/or rotational [33, 34] movements during opening and closing, and such movements could increase or decrease the accessibility of individual side-chains independent of overall pore dimensions. Furthermore, residues close to the extracellular "gate" might show strongly state-dependent accessibility resulting from gate movement [8]. In addition, movement of other parts of the outer pore (such as TM8 [11]) could influence access to the outer pore during channel gating.

Our results suggest that dynamic conformational changes of the outermost part of the Cl^- permeation pathway take place as the channel opens and closes (Fig. 7a, d). While the extent of these conformational changes cannot be discerned from our present study, large-scale rearrangements of the extracellular face of the protein are not predicted from structures of the channel in inactive) (Fig. 7b) and near-open states (Fig. 7c). Of course, since the structure shown in Fig. 7c remains closed at its extracellular end, it is possible that a further, local conformational rearrangement is associated with the final channel opening step and that this could be associated with a relative separation of the outer ends of TMs 1, 6, and 12 as predicted by our results. Furthermore, our results suggest that, even if they are relatively minor, conformational changes at the outer mouth of the pore are important for channel opening, since manipulations that prevent these changes (such as Cd^{2+} bridge formation) appear sufficient to stabilize a non-conducting state of the channel. A simple cartoon model of pore opening and closing based on these results is shown in Fig. 7d. In this model, separation of the outer ends of the TMs leads to opening of an extracellular gate [3, 8, 11, 14] and widening of the outer mouth of the pore. This model is consistent with the suggestion, based on cryo-EM structures, that the outer TMs undergo a rigid-body movement during channel gating [11]. Disulfide bond and/or metal bridge formation has previously been reported between more central and cytoplasmic parts of TMs 1 and 6 [13, 27, 35, 36], 1 and 12 [13, 36], and 6 and 12 [13, 18, 19, 36], suggesting that these core components of the pore remain in relatively close proximity throughout the pore, at least at some point in the gating cycle. Interestingly, metal bridge formation has suggested that the central and inner parts of TMs 6 and 12 may also separate when the channel opens, whereas the corresponding parts of TMs 1 and 12 have been suggested to move closer together on channel opening [13, 36], potentially pointing to region-specific differences in inter-TM movements during channel gating.

Since we were unable to identify any disulfide bonds or metal bridges between different TMs that appeared capable of stabilizing the channel in a conducting, open state, our results do not directly suggest a mechanism by which manipulation of outer pore mouth structure by potentiator drugs might increase channel activity. In theory, if channel closure is associated with these TMs moving together, then a physical manipulation that could hold them apart might be predicted to stabilize the channel open state. However,

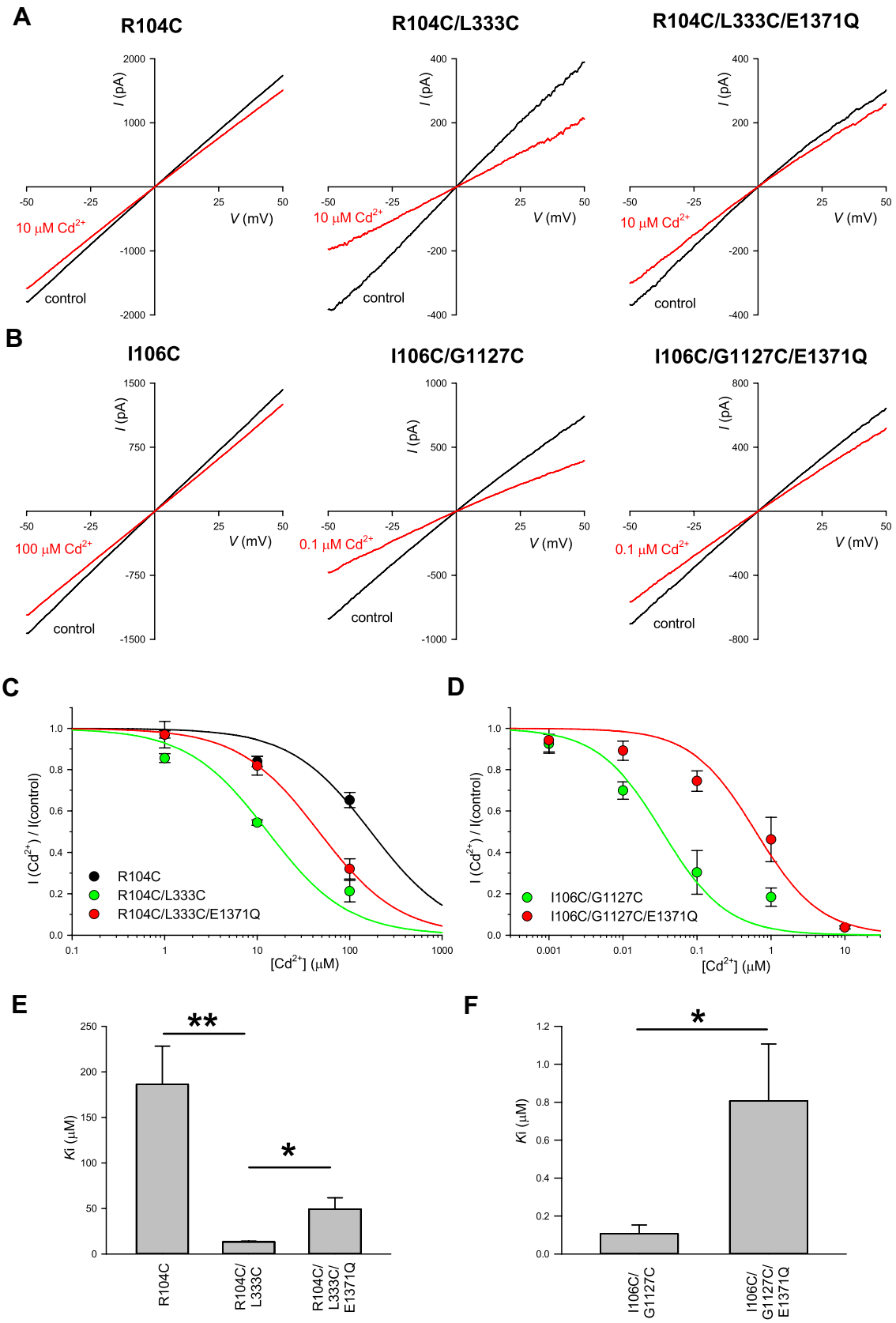
A
R104C
R104C/L333C
R104C/L333C/E1371Q
I (pA)
V (mV)
10 μM Cd2+
control
B
I106C
I106C/G1127C
I106C/G1127C/E1371Q
100 μM Cd2+
0.1 μM Cd2+
C
D
I (Cd2+) / I(control)
[Cd2+] (μM)
R104C
R104C/L333C
R104C/L333C/E1371Q
I106C/G1127C
I106C/G1127C/E1371Q
E
F
Ki (μM)
**
*
R104C
R104C/ L333C
R104C/ L333C/ E1371Q
I106C/ G1127C
I106C/ G1127C/ E1371Q

◂**Fig. 6** State-dependent metal bridge formation between the outer end of TM1 and TMs 6 or 12. **a**, **b** Example whole-cell *I–V* relationships for the named channel variants. Each was recorded before (control; black lines) and after (red lines) addition of Cd^{2+} (at the concentrations indicated) to the extracellular solution. **c**, **d** Mean fraction of control current remaining following addition of different concentrations of Cd^{2+} to the extracellular solution for the different channel variants indicated. Mean data have been fitted as described in "Materials and methods". **e**, **f** Mean K_i values estimated from fits to data from individual cells exposed to different concentrations of Cd^{2+}. Note that the apparent Cd^{2+} affinity of I106C was too low for quantification. Asterisks indicate a significant difference between the groups indicated (*$p < 0.05$; **$p < 0.01$). Mean of data from 3 to 4 cells in **c**–**f**

how this could be achieved by a small molecule without physical occlusion of the outer mouth of the pore is not clear. Alternatively, as the outer ends of these TMs separate during channel opening, this separation movement might bring these TMs into closer proximity with other parts of the protein, for example, other TMs or ECLs that are more peripheral from the pore mouth. If so, it might be predicted that stabilization of these other putative associations could, in theory, stabilize the channel open state and, therefore, provide the possibility for channel potentiation.

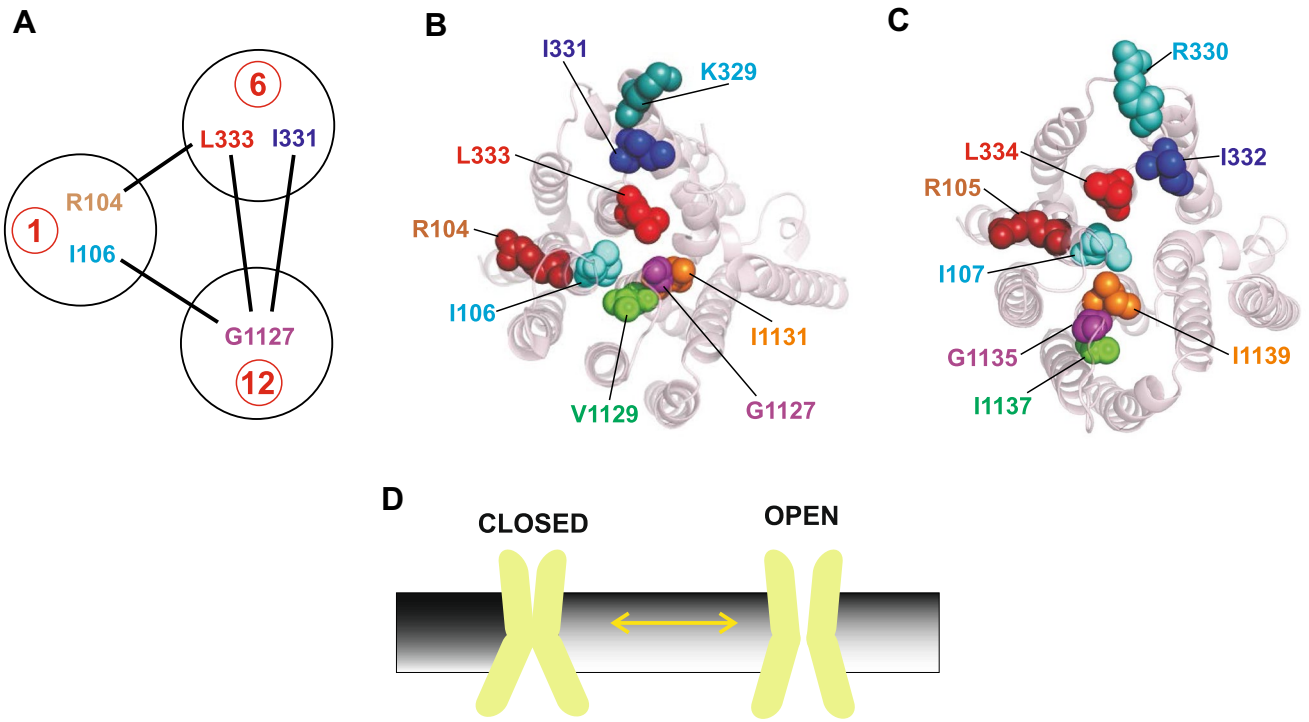

Fig. 7 Conformational changes in the outer pore during opening and closing. **a** Disulfide bond formation (Figs. 2, 3, 4) and Cd^{2+} bridge formation (Figs. 5, 6) suggests that side-chains in TM1 (R104, I106), TM6 (I331, L333) and TM12 (G1127) are in close proximity in closed channels (as indicated by lines drawn between individual residues) and move apart as the channel opens. Location of residues studied on the extracellular surface of CFTR in the inactive state (**b**) and in the "near-open" state (**c**) (as shown in Fig. 1), viewed from the extracellular side of the membrane. Because **c** is zebrafish CFTR, the numbering of individual amino acids is slightly different. According to these structures, on average, residues in TMs 1 and 6 are closer together in the "near-open" state than in the inactive state; those in TMs 1 and 12 are closer together in the "near-open" state than in the inactive state; and those in TMs 6 and 12 are closer together in the inactive state than in the "near-open" state. **d** Simple cartoon model of CFTR pore opening based on the present results. Separation of the extracellular ends of the TMs results in opening of a gate and widening of the outer mouth of the pore. This model is consistent with the suggestion, based on cryo-EM structures, that the extracellular parts of the protein undergo a rigid-body movement during channel opening and closing [11]

Acknowledgements We would like to thank Christina Irving for technical assistance. This work was supported by Cystic Fibrosis Canada.

References

1. Bosch B, De Boeck K (2016) Searching for a cure for cystic fibrosis. A 25-year quest in a nutshell. Eur J Pediatr 175:1–8
2. Zegarra-Moran O, Galieta LJV (2017) CFTR pharmacology. Cell Mol Life Sci 74:117–128
3. Linsdell P (2017) Structural changes fundamental to gating of the cystic fibrosis transmembrane conductance regulator anion channel pore. Adv Exp Med Biol 925:13–32
4. Callebaut I, Hoffmann B, Mornon J-P (2017) The implications of CFTR structural studies for cystic fibrosis drug development. Curr Opin Pharmacol 34:112–118
5. Chin S, Hung M, Bear CE (2017) Current insights into the role of PKA phosphorylation in CFTR channel activity and the pharmacological rescue of cystic fibrosis disease-causing mutants. Cell Mol Life Sci 74:57–66
6. Moran O (2017) The gating of the CFTR channel. Cell Mol Life Sci 74:85–92
7. Sorum B, Czégé D, Csanády L (2015) Timing of CFTR pore opening and structure of its transition state. Cell 163:724–733
8. Gao X, Hwang T-C (2015) Localizing a gate in CFTR. Proc Natl Acad Sci USA 112:2461–2466
9. Wei S, Roessler BC, Icyuz M, Chauvet S, Tao B, Hartman JL, Kirk KL (2016) Long-range coupling between the extracellular gates and the intracellular ATP binding domains of multidrug resistance protein pumps and cystic fibrosis transmembrane conductance regulator channels. FASEB J 30:1247–1262
10. Liu F, Zhang Z, Csanády L, Gadsby DC, Chen J (2017) Molecular structure of the human CFTR ion channel. Cell 169:85–95
11. Zhang Z, Liu F, Chen J (2017) Conformational changes of CFTR upon phosphorylation and ATP binding. Cell 170:483–491
12. Tordai H, Leveles I, Hegedüs T (2017) Molecular dynamics of the cryo-EM CFTR structure. Biochem Biophys Res Commun 491:986–993
13. El Hiani Y, Linsdell P (2014) Metal bridges illuminate transmembrane domain movements during gating of the cystic fibrosis transmembrane conductance regulator chloride channel. J Biol Chem 289:28149–28159
14. Linsdell P (2017) Architecture and functional properties of the CFTR channel pore. Cell Mol Life Sci 74:67–83
15. Zhang Z-R, Song B, McCarty NA (2005) State-dependent chemical reactivity of an engineered cysteine reveals conformational changes in the outer vestibule of the cystic fibrosis transmembrane conductance regulator. J Biol Chem 280:41997–42003
16. Beck EJ, Yang Y, Yaemsiri S, Raghuram V (2008) Conformational changes in a pore-lining helix coupled to cystic fibrosis transmembrane conductance regulator channel gating. J Biol Chem 283:4957–4966
17. Wang W, Linsdell P (2012) Alternating access to the transmembrane domain of the ATP-binding cassette protein cystic fibrosis transmembrane conductance regulator (ABCC7). J Biol Chem 287:10156–10165
18. Wang W, Linsdell P (2012) Relative movements of transmembrane regions at the outer mouth of the cystic fibrosis transmembrane conductance regulator channel pore during channel gating. J Biol Chem 287:32136–32146
19. Zhou J-J, Li M-S, Qi J, Linsdell P (2010) Regulation of conductance by the number of fixed positive charges in the intracellular vestibule of the CFTR chloride channel pore. J Gen Physiol 135:229–245
20. Mense M, Vergani P, White DM, Altberg G, Nairn AC, Gadsby DC (2006) In vivo phosphorylation of CFTR promotes formation of a nucleotide-binding domain heterodimer. EMBO J 25:4728–4739
21. Li M-S, Demsey AFA, Qi J, Linsdell P (2009) Cysteine-independent inhibition of the CFTR chloride channel by the cysteine-reactive reagent sodium (2-sulphonatoethyl) methanethiosulphonate. Br J Pharmacol 157:1065–1071
22. Zhou J-J, Fatehi M, Linsdell P (2008) Identification of positive charges situated at the outer mouth of the CFTR chloride channel pore. Pflügers Arch 457:351–360
23. Fatehi M, Linsdell P (2009) Novel residues lining the CFTR chloride channel pore identified by functional modification of introduced cysteines. J Membr Biol 228:151–164
24. Gao X, Bai Y, Hwang T-C (2013) Cysteine scanning of CFTR's first transmembrane segment reveals its plausible roles in gating and permeation. Biophys J 104:786–797
25. Vergani P, Nairn AC, Gadsby DC (2003) On the mechanism of MgATP-dependent gating of CFTR Cl^- channels. J Gen Physiol 121:17–36
26. Broadbent SD, Wang W, Linsdell P (2014) Interaction between two extracellular loops influences the activity of the cystic fibrosis transmembrane conductance regulator chloride channel. Biochem Cell Biol 92:390–396
27. Negoda A, El Hiani Y, Cowley EA, Linsdell P (2017) Contribution of a leucine residue in the first transmembrane segment to the selectivity filter region in the CFTR chloride channel. Biochim Biophys Acta 1859:1049–1058
28. Linsdell P (2015) Metal bridges to probe membrane ion channel structure and function. Biomol Concepts 6:191–203
29. Holmgren M, Shin KS, Yellen G (1998) The activation gate of a voltage-gated K^+ channel can be trapped in the open state by an inter-subunit metal bridge. Neuron 21:617–621
30. Heymann G, Dai J, Li M, Silberberg SD, Zhou H-X, Swartz KJ (2013) Inter- and intrasubunit interactions between transmembrane helices in the open state of P2X receptor channels. Proc Natl Acad Sci USA 110:E4045–E4054
31. Zhou Y, Xia X-M, Lingle CJ (2015) Cadmium-cysteine coordination in the BK inner pore region and its structural and functional implications. Proc Natl Acad Sci USA 112:5237–5242
32. Corradi V, Vergani P, Tieleman DP (2015) Cystic fibrosis transmembrane conductance regulator (CFTR): closed and open state channel models. J Biol Chem 290:22891–22906
33. Bai Y, Li M, Hwang T-C (2010) Dual roles of the sixth transmembrane segment of the CFTR chloride channel in gating and permeation. J Gen Physiol 136:293–309
34. Bai Y, Li M, Hwang T-C (2011) Structural basis for the channel function of a degraded ABC transporter, CFTR (ABCC7). J Gen Physiol 138:495–507
35. Wang W, El Hiani Y, Linsdell P (2011) Alignment of transmembrane regions in the cystic fibrosis transmembrane conductance regulator chloride channel pore. J Gen Physiol 138:165–178
36. Gao X, Hwang T-C (2016) Spatial positioning of CFTR's pore-lining residues affirms an asymmetrical contribution of transmembrane segments to the anion permeation pathway. J Gen Physiol 147:407–422